Computational Modelling of Integrin Interactions Under an Electric Field

A Thesis

submitted to

Indian Institute of Science Education and Research Pune in partial fulfilment of the requirements for the BS-MS Dual Degree Programme

by

Abhay N

Indian Institute of Science Education and Research Pune

Dr. Homi Bhabha Road,

Pashan, Pune 411008, INDIA.

April, 2025

Supervisor: Prof. Bikramjit Basu, Materials Research Centre, IISc

Name: Abhay N, Chemistry Department, IISER Pune

Certificate

This is to certify that this dissertation entitled Computational Modelling of Integrin Interactions Under an Electric Field towards the partial fulfilment of the BS-MS dual degree programme at the Indian Institute of Science Education and Research, Pune represents study/work carried out by Abhay N at the Indian Institute of Science under the supervision of Bikramjit Basu, Professor, Materials Research Centre, Indian Institute of Science during the academic year 2024-2025.

Name & signature of your Guide

Name: Prof. Bikramjit Basu

This thesis is dedicated to my family and Room 249

Declaration

I hereby declare that the matter embodied in the report entitled "Computational Modelling of Integrin Interactions Under an Electric Field", are the results of the work carried out by me at the Department of Chemistry, Indian Institute of Science Education & Research (IISER) Pune, under the supervision of Prof. Bikramjit Basu and the same has not been submitted elsewhere for any other degree. Wherever others contribute, every effort is made to indicate this clearly, with due reference to the literature and acknowledgement of collaborative research and discussions.

Name & Signature of Student

Name: Abhay N

Roll #: 20201171

Acknowledgments

First, I would like to thank Prof. Bikramjit Basu for always providing me with his invaluable advice and also mentoring me and helping me through every step of my MS project. I would also like to thank Dr. Subhadip Basu and Prof. Aurelie Carlier for helping me with a lot of the doubts I had in this project and providing me with support when it was required.

I am grateful to the Kishore Vaijnanik Protsahan Yojana (KVPY), DST, Government of India, for the fellowship. I am also grateful to IISc and in particular, the Materials Research Centre (MRC) for hosting me and providing me with all the necessary resources for my thesis.

I would also like to thank my labmates Susantika, Bijay, Dhrmendra, Dr. Sulob, Dr. Deepa, Shruthi, Rishad, Sriprakash and Krittika for being a constant support in the lab.

Finally, I would like to thank my friends Prabhav and Avaneesh for being extremely supportive during my days in Bengaluru and also my parents and grandparents who have taken care of me during tough times. Special thanks to Shrivatsa, Vasu, Ayush, Neharwal, Pratham, Anwesha, Amogha, Shrey, Ujwal and Prasanna for being one of the greatest friends during my entire BS-MS journey.

Table of Contents

List of Tables

List of Figures

Abstract

Cell-material interactions involve the adsorption of proteins on material surfaces followed by biophysical interactions among adsorbed proteins and cell surface integrins. Molecular Dynamics (MD) simulations have been employed to gain atomistic insights into these complex phenomena with varying degrees of success. While MD studies on protein adsorption on material surfaces have gained significant traction, such studies on integrin-protein interactions within the extracellular space remains limited. This work aims to address this gap by providing mechanistic insights into the extracellular integrin-fibronectin interactions through the analysis of interaction energies and factors indicative of stability, such as root mean square deviation (RMSD) and centre-of-mass distance between interacting proteins. Moreover, higher affinity interactions between fibronectin and integrin will be reflected in the larger number of contacts established between them. Following this, kinetic modelling was conducted to investigate the effects of an electric field on focal adhesion complexes (FACs) using a coarse-grained ab-initio kinetic model. The results from this study reveal that the impact of the electric field on the concentration of mature adhesions is only observable at high field strengths. Further analysis indicates that the total force exerted by focal adhesions exhibits a more pronounced dependence on electric field strength. Additionally, a smaller number of vinculins are recruited into the FACs under high-field conditions. The mean actin retrograde velocity is also observed to increase with electric field strength, thereby impacting cell traction and downstream signalling pathways.

Chapter 1 Introduction

Cell – material interactions play a key role in the biocompatibility and clinical applications of biomaterials, implants and scaffolds. The first step in these interactions is the protein adsorption onto the material substrate. This important step is facilitated by the interaction of the cell-surface receptors integrins[1], which enable the adsorption[2] of proteins onto any surface[3]. Such interactions also involve adhesive glycoproteins such as fibronectin, which facilitate the cell adhesion to the substrate, as shown in Fig 1.

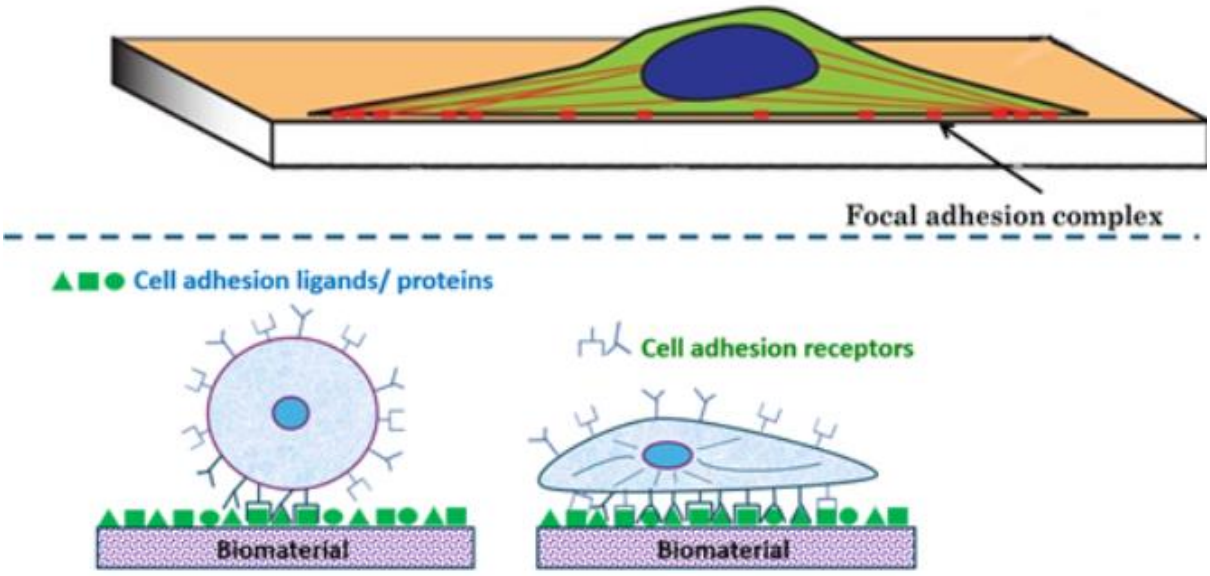

i. Fig 1a: Formation of Focal Adhesions and the role of cell adhesion receptors such as integrin in cell – biomaterial interactions

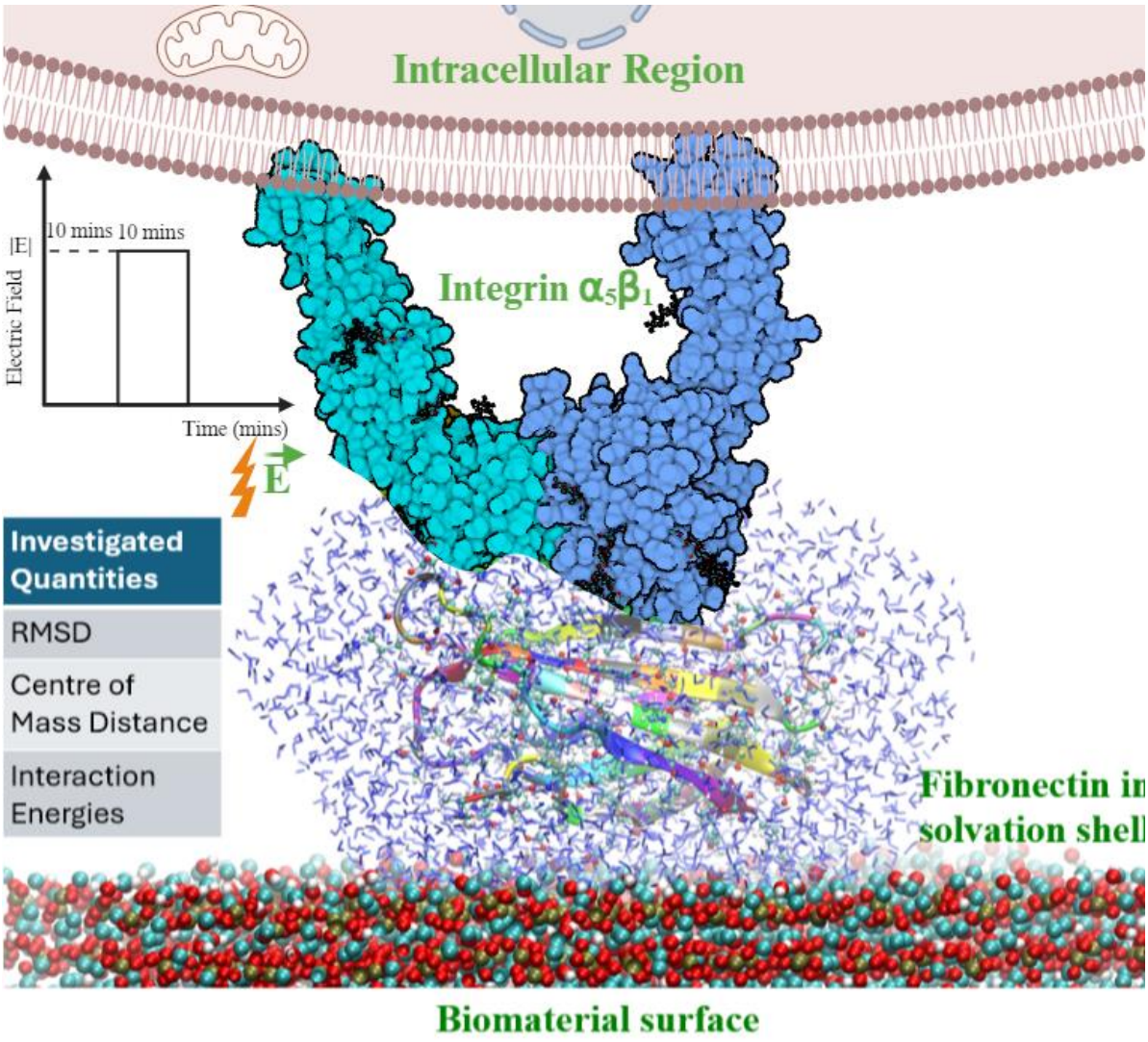

ii. Fig 1b: The system of the cell surface receptor integrin α5β1 bound to the biomaterial substrate with the help of fibronectin protein, adsorbed on a biomaterial substrate, in a solvation shell. The integrin or protein structure is not shown to scale. The electrical stimulation protocol is also shown. An electric field is being applied perpendicular to the cell surface. (Created in BioRender.com)

Cell - material interaction process begins with protein adsorption onto the material substrate. This process is facilitated by a class of trans – membrane proteins called integrins, which bind to surface proteins that serve as receptors for cell-surface adhesion. These integrins enable cells to interact with surfaces and facilitate movement or interactions between cells and biomaterials. Adherence is also mediated through fibronectin, which functions as an adhesive protein in various contexts. Fibronectin binds directly to the biomaterial itself, and to integrin, enhancing cell adhesion and ensuring proper integration into the biological environment. Fibronectin binds directly to the biomaterial itself, and to integrin, enhancing cell adhesion, while ensuring better cell – material interactions. A key

component of this interaction is the binding of the integrin to fibronectin. Over the last decade, our research group, using experimental and computational approaches, has investigated the biophysical origin of tailored electrical stimuli-directed differentiation of bone-marrow derived stem cells into bone, cardiac, glial, neuron-like cells with clinically desired electrophysiological functionality[4,5,6,7,8,9,10,11]. In rationalising these experimental observations, the research group has also conducted MD simulations and analytical studies to develop quantitative insights into the cell fate changes[2,12,13,18,14]. These studies are particularly useful to quantitatively analyse bioelectric stresses in and around cells as well as kinetics of protein adsorption.

As far as the underlying biophysical mechanisms are concerned, Electric Field stimulation has been found to indirectly influence key biochemical pathways such as the YAP/TAZ signalling pathway, which regulates cell growth, embryonic development, and cancer[15]. Such stimulation has also been shown to promote differentiation of mesenchymal stem cells into neuronal cells[16]. In a comprehensive theoretical work, Cheng et al.[17] reviewed a number of mathematical models, in the context of the interaction of biophysical cues to cells. These biophysical cues can be related to either dynamic strain, mechanical force, matrix rigidity, shear stress etc. We assume that the electric field stimuli are present in the form of bioelectric stress, which act as biophysical cues to regulate the cell fate processes. Hence, it is essential to probe into these phenomena at the molecular level, which has been one of the main objectives of this study.

The present work has been divided into two parts. The first part aims to analyse the results of Molecular Dynamics (MD) simulation of the integrin $\alpha_5\beta_1$ with the 9^{th} – 10^{th} repeats of the Fibronectin III (FN III). The binding dynamics of fibronectin to the integrin in the extracellular portion has been studied in the absence and presence of an external electric field. The second part of the work focusses on the intracellular portion of the process, when an electric field is applied. The key components of focal adhesions, containing the intracellular portion of the integrin, talin and vinculin have been studied, based on a kinetic model proposed by Honasoge et al.[22] The formation of focal adhesions and the actin retrograde velocity have been the key parameters that have been studied.

1.1 Extracellular region

The first part of the study focusses on the extracellular portion and consists of the extracellular portion of integrin $\alpha_5\beta_1$ with the 9^{th} – 10^{th} repeats of Fibronectin III (FN III), in a bound state. Here, the focus is on finding the stability of the complex in terms of binding energy of the two proteins, with varying electric field magnitudes and directions. The binding site of the protein consists of the RGD amino acid sequence, consisting of the amino acids Arginine (R), Glycine (G) and Aspartic Acid(D) which binds to the metal centres containing Mn^{2+} ions, in between the α_5 and β_1 subunits of the integrin, known as the Metal Ion–Dependent Adhesion Site (MIDAS) and adjacent to the MIDAS (ADMIDAS) centres. While traditionally, MIDAS and ADMIDAS sites have been found to contain Ca^{2+} and Mg^{2+} ions in experimental studies, it has been established that these ions highly favour a closed structure of the integrin, which hides the binding sites of the fibronectin. However, the Mn^{2+} ions tend to favour the open structure of the integrin, which facilitates the binding of the 10^{th} repeat of FN III to it through the RGD sequence. Another site on the 9^{th} repeat of FN III, having the amino acid sequence PHSRN, has been experimentally found to facilitate binding with the integrin as well. In the RGD sequence, the arginine and aspartic acid residues are actively involved in bonding with the metal centres and glycine acts as an anchor for the two residues. The binding sites on the integrin, along with the metal sites, include the residues Lysine and Aspartic Acid, as seen in Fig 2.

Multiple MD simulations were conducted on the given system, with electric field strengths ranging from 0 – 1 V/nm, and electric fields being applied from three orthogonal directions. The timescale of the simulations were 50 ns.

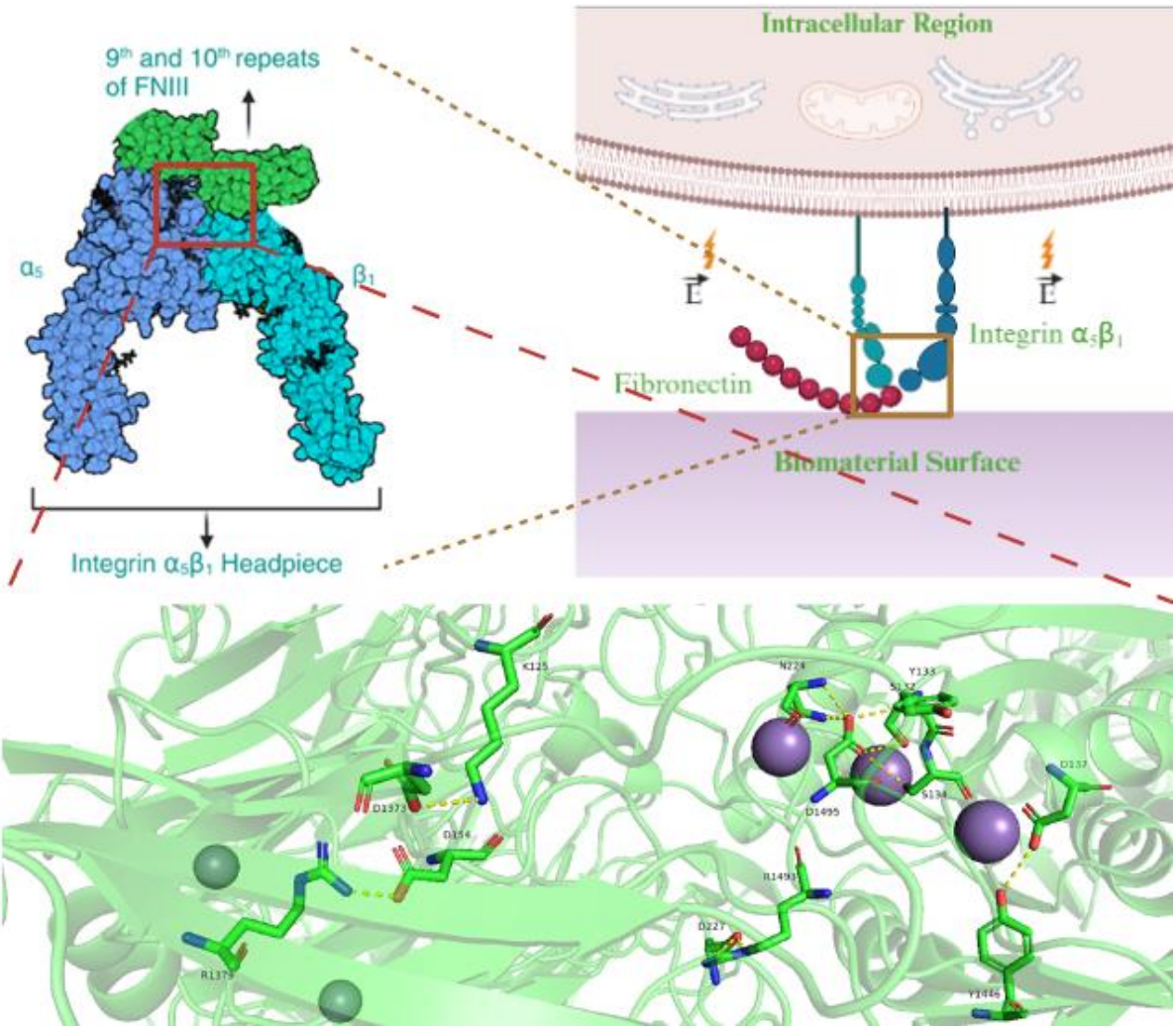

iii. Fig 2: The initial structure used for the MD simulation. The 9th and 10th repeats of Fibronectin III is bound to the site in between the α5 and β1 subunits of the Integrin (Created in BioRender.com)

1.2 Intracellular region

The second part of the work focusses on the formation of focal adhesions, which help in cell adhesion to a biomaterial surface. Focal adhesions consist of the intracellular portion of the aforementioned integrin, along with two adaptor proteins, namely talin (Tal) and vinculin (Vin). Focal adhesions (FAs) are formed by a number of assemblies of these proteins, known as Integrin-Adaptor Protein complexes (IAPCs). Each FA can contain IAPCs consisting of 2 or 3 vinculins. These are formed by the maturation, of Nascent Adhesions (NAs), which are formed by an aggregation of IAPCs containing just 1 vinculin. Hence, FAs are formed by recruiting subsequent vinculins to NAs. The base model is based on a model by Swaminathan

et al.[29] called the molecular clutch mode (see Fig 3). In this particular model, the focal adhesions are modelled as a system of Hookean springs, where the total stiffness of the focal adhesions have contributions from the stiffness of the substrate, the integrin, talin and all the vinculins. The cytoskeleton applies a force on the focal adhesions using Myosin motors, which are attached to actin filaments. The force causes the monomer segments in the actin polymer to polymerize on one end and depolymerize on the other end. This causes an apparent motion of the actin filament, known as retrograde motion. The vinculins in the FAs are capable of binding to the actin in the cytoskeleton and can thus influence cell the actin retrograde velocity, which influences the cell traction. This has been reported to influence the aforementioned YAP/TAZ pathway, and other such biochemical pathways[18]. A similar approach has been carried out in this work, where the electric field has been integrated into the model and has been varied instead of substrate stiffness. This study has attempted to quantitatively analyse the effects of the electric field stimulation on the formation of FAs from NAs by using a pre-existing kinetic model as proposed by Honasoge et al[28], which has been successfully implemented to analyse the effects of substrate stiffness on FA maturation. This model also hypothesizes a signalling molecule that influences the formation of FAs from NAs. Since the model is coarse grained, it only considers FAs and NAs to be formed as an aggregation of 25 or 50 IAPCs, which have been termed as seeds and clusts respectively. The force due to an external electric field has been incorporated by using the charges of the proteins present in focal adhesions, incorporated into the pulling force from the actin using the myosin motors.

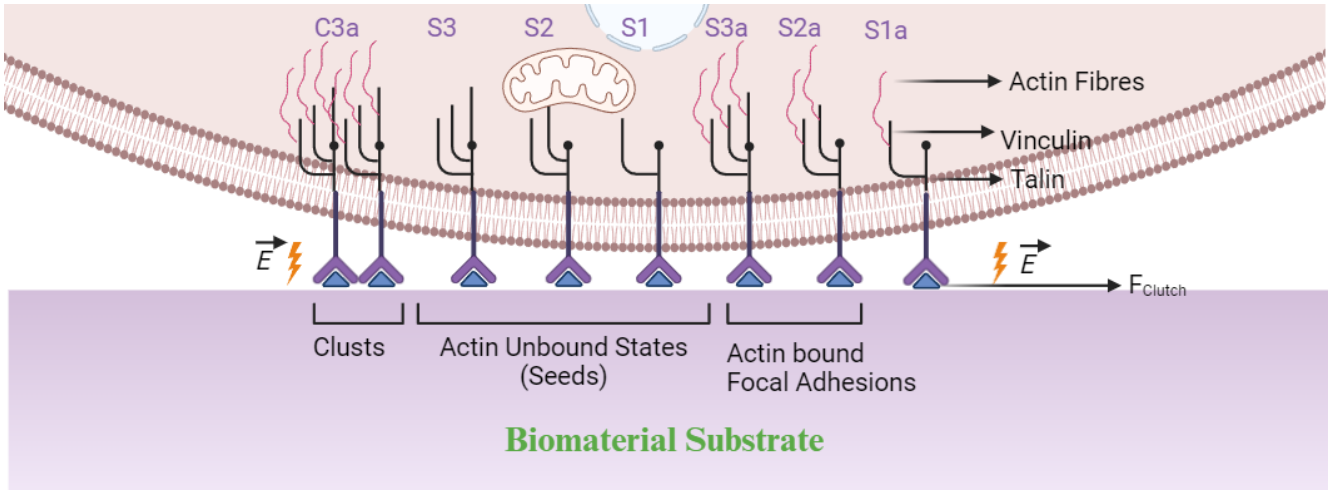

iv. Fig 3: Schematic of the Formation of clutches considered in the kinetic model along with the forces being applied on the species (Created in BioRender.com)

Overall, the present work aims to provide a comprehensive understanding of the events of cell adhesion to a materials surface in the presence of an electric field, considering both the intracellular and extracellular effects of an external electric field. Finally, the work has put together quantitative simulation efforts to establish the role of an external field in some of the important processes, such as the change in actin retrograde velocity and the binding dynamics of integrins to fibronectin.

Chapter 2 Materials and Methods

2.1 MD Simulation

2.1.1 System Preparation

The first step of the Molecular Dynamics (MD) Simulations was cleaning up the PDB structure with id 7NWL[19]. The protein structure is obtained from a Cryo-EM configuration of the 7^{th}-10^{th} repeats of Fibronectin bound to the Integrin $\alpha_5\beta_1$. A bunch of different antibodies are also present in the structure, which function in stabilizing the whole protein for Cryo-EM characterization. These antibodies were removed from the obtained PDB structure along with the 7^{th} and 8^{th} repeats of FN III, which were irrelevant for the binding dynamics in the simulation as part of the cleaning process. The initial structure contains the integrin $\alpha_5\beta_1$, bound to the 9^{th} and 10^{th} repeats of Fibronectin III. These domains have been known to be important for interactions with the integrin, the RGD sequence[20] in the 10^{th} repeat being the primary binding site. The integrin portion contains 1042 residues while the fibronectin portion contains 180 residues. The initial structure was kept inside a simulation box with dimension 9.8 x 9.8 x 9.8 nm^3. The system was first solvated with TIP3P water. Counter ions K^+ and Cl^- were added to make the system charge neutral and to maintain the physiological salt concentration of 0.15. The total number of water molecules was 205,604 and the system contains a total of 636,210 atoms. This initial structure was prepared using CHARMM-GUI.[21, 22]

2.1.2 Simulation Parameters

Energy Minimization was done on GROMACS 2024.3[23] with the steepest descent algorithm for 10000 steps. Subsequent equilibration was performed in NVT and NPT ensemble, each for 2 ns, at 300K temperature and 1 bar pressure for 2ns each with position restraints on the protein. The time step used for these equilibration runs were 1fs. The thermostat was chosen to be velocity rescale[24] with coupling constant of 1ps and the barostat was C-rescale[25] with coupling constant of 5ps. The equilibrated system was then subjected to production runs for 50 ns.

Production MD simulation was conducted in a NPT ensemble with the same thermostat and barostat, with time step of 4fs.LINCS[26] algorithm was used to

constraint H-bonds and hydrogen mass repartitioning[27] was applied. Particle Mesh Ewald was used for long range electrostatics. AMBER99SB-ILDN[28] force field was chosen for the simulation. Finally, the critical analysis of MD simulation data was done with various GROMACS modules and visualization was done with VMD[29] software.

Multiple MD runs were performed with electric field strengths ranging from 0 to 1000 MV/m, and the system response along three orthogonal directions were investigated for electric field strength values of 5 and 10 MV/m. The nature of the electric field was a constant DC current. The upper bound value is close to the values of electric field strength where the fibronectin binding was found to be on the verge of instability without denaturation. These extra simulations were performed to investigate the directional effects of the external electric field. After establishing relative invariance when it comes to the direction of the external electric field, MD simulations were conducted along the given directions as shown in table 1.

Electric field Direction	**Electric Field Strength (MV/m)**
x	1000
z	500
y	250
x	100
z	50
x	10
y	5
z	1

Table 1: Electric field strengths and directions used for MD Simulation study.

2.2 Kinetic Modelling

The kinetic model was based on the work published by Honasoge et al[30]. The system of an integrin with the intracellular adaptor proteins – Talin and Vinculin were modelled as a system of springs based on the molecular clutch model by Swaminathan et al[31]. All these clutches were classified based on the number of Vinculins contained in them (1, 2 or 3) and also on whether they were actin bound, or

unbound states, as shown in Fig 3. The total simulation time was 20 minutes, and the electric field was applied 10 minutes after the start of the simulation. Euler's forward integration method was used to solve the differential equations with a time step of 5 ms.

Model assumptions:

a) The clutches are modelled as a setup of springs, with the force exclusively from actin pulling, which arises from the myosin motors and the external electric field.
b) First-order clutches with one vinculin are said to be Nascent Adhesions (NAs), which recruit more vinculin to form mature higher-order Focal Adhesions (FAs), with two or three vinculins.
c) 50 Integrin-Adaptor Protein Complexes (IAPCs) are theorized to form adhesions called clusts.
d) These are theorized to be formed by 2 sets of 25 IAPCs called seeds.
e) Time Dependent Rate Modifications have been applied to account for changes in rate constants with changes in force.
f) Integrin-Talin(catch-slip) and Talin-actin(slip) bonds are said to rupture as a result of reaching certain force thresholds.
g) Initial concentration of integrins, talin and vinculin is assumed to be 1 micromolar and rest 0.
h) Vinculin is assumed to be abundant in cytoplasm and have a constant concentration throughout.
i) All proteins are assumed to be point charges under the application of an electric field.
j) The force due to the electric field is assumed to be additive to the force by the myosin motors.

Multiple factors of the system in have been considered for the kinetic model. These include the following processes:

a) Formation and dissociation of individual IAPCs from individual integrin, talin and vinculins
b) Aggregation of 25 IAPCs to form subsequent seeds and dissociation of seeds to form individual IAPCs
c) Dimerization of seeds to form clusts and splitting of clusts to form seeds

d) Binding and Unbinding of Actin to the Seeds and Clusts involved in the formation of force-dependent clutches
e) Unfolding and refolding of Talin, which can increase and decrease the vinculin binding sites respectively, which changes the order of the clutches
f) Signalling molecules present in such a process like Focal Adhesion Kinase (FAK) and Extracellular Regulated Kinases (ERK) play an essential role in stopping indefinite formation of FAs from NAs.
g) These signalling molecules are modelled in the form of a Signal Dependent Rate Modification.

The kinetic model of Honasoge et al.[22] was modified by adding an electric force to the total force on these clutches by the following equation:

$$\boldsymbol{F_{Total}} = \boldsymbol{F_{clutch}} + \boldsymbol{F_{electric}} \quad \text{---------- (1)}$$

Where $\boldsymbol{F_{electric}} = \boldsymbol{qE}$, where q is the charge on the protein and E is the electric field and $\boldsymbol{F_{clutch}}$ is the pulling force of actin by the myosin motors.

This F_{Total} was then incorporated into the rate equations in the form of force dependent rate constants, which will influence the evolution of the rate equations $\boldsymbol{F_{Total}}$ can directly cause certain events like the unfolding of Talin or the disassembly of these clutches resulting in the unbinding of Actin, resulting in the total force of the clutches being only due to the electric field. So, in essence, these forces are directly affected by the electric field which in turn, affect observable quantities like the clutch concentration and actin retrograde velocity. The actin retrograde velocity is given by:

$$v_{retro} = v_u.\left(1 - \frac{F_{Total}}{F_{Myo}}\right) \quad \text{---------- (2)}$$

where v_u is the unload velocity of actin filaments F_{Total} is the total force exerted by actin-bound clutches and F_{Myo} is the total force exerted by myosin motors.

Chapter 3 Results

3.1 Integrin – Fibronectin Interactions

For analysing the MD simulation results, various quantities were calculated with different values of a constant electric field applied from different directions. First, directional invariance was established by analysing the effects of the same electric field applied from different orthogonal directions. Moreover, the electric field values considered in this study are extremely high to produce an overexaggerated response to electric field in such small timescales. Since it is not practical experimentally, the results are more qualitative than quantitative. This is also due to the fact that the production simulations were conducted for a small amount of time, which is 50 ns. The effects of longer timescales were also not explored in this study, owing to limited computational resources.

3.1.1 Establishing Directional Invariance

First, directional invariance was established by conducting simulation from there different orthogonal directions with the same electric field strength. It was observed that the calculated quantities like Root Mean Square Deviations (RMSD) and interaction energies for both the integrin and fibronectin did not vary with change in direction. These quantities were mainly calculated for electric field strengths where it was presumed that the binding between the integrin and fibronectin would be stable.

First, the quantities were calculated at an electric field strength of 5 MV/m. The three investigated orthogonal directions have been loosely named as the x, y and z-directions, from which, constant electric field was applied. As seen in Fig 4, the RMSD values of both the integrin and fibronectin did not vary much with direction and stayed consistently close to 0 nm over the course of the simulation. There was a slightly higher variation in the interaction energies observed between the integrin and fibronectin. In particular, the interaction energy when the electric field was applied in the x-direction was almost consistently the lowest as seen in Fig 4, at around -800 kJ/mol as compared to about -600 kJ/mol for a 0 electric field. However, it was observed that the protein eventually tumbled into a position with the lowest energy as seen by the screenshots in Fig 5.

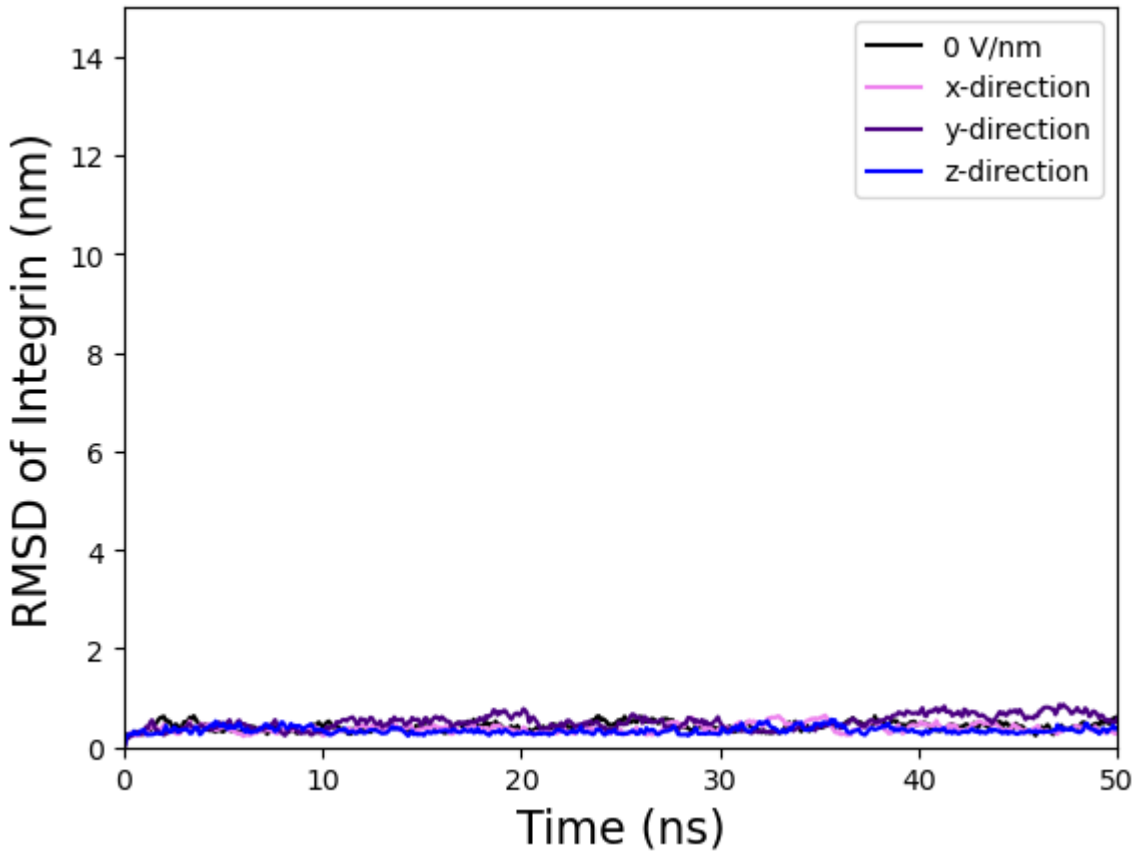

v. Fig 4a: RMSD values of the integrin when an electric field of 5 MV/m is applied in three different directions.

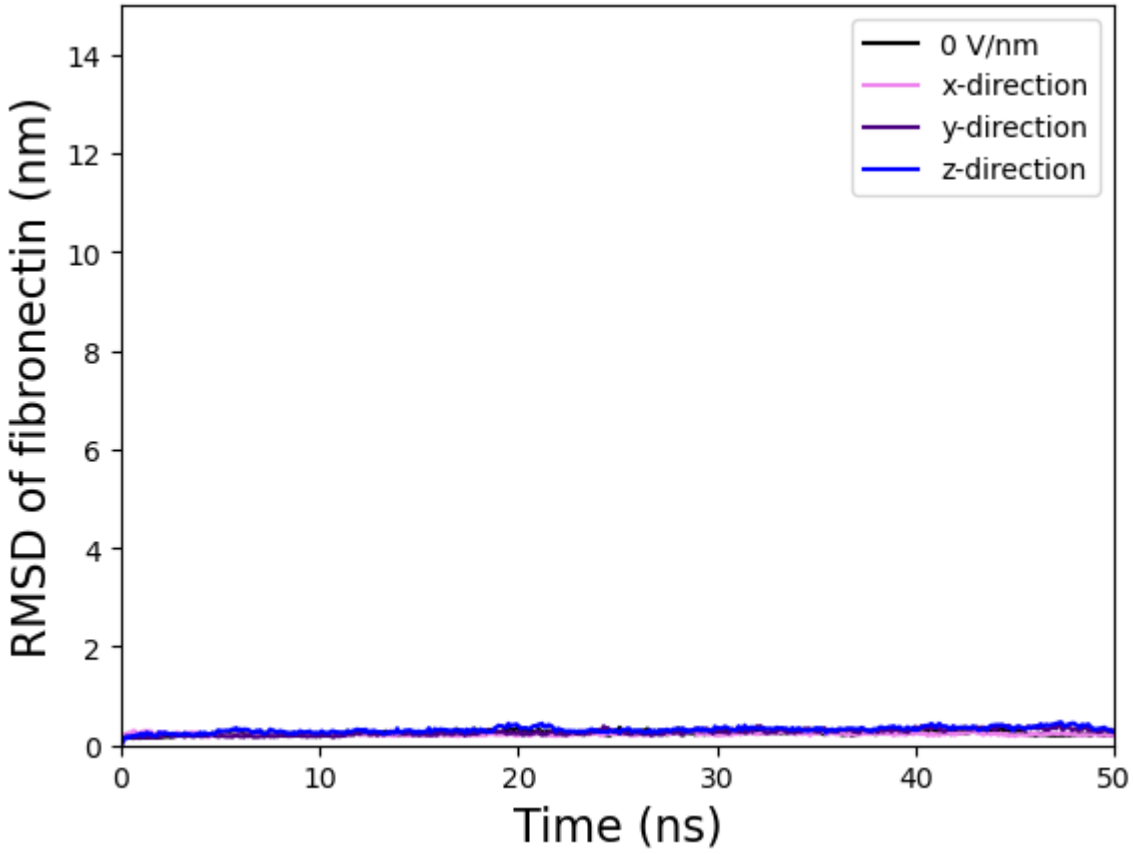

vi. Fig 4b: RMSD values of fibronectin when an electric field of 5 MV/m is applied in three different directions.

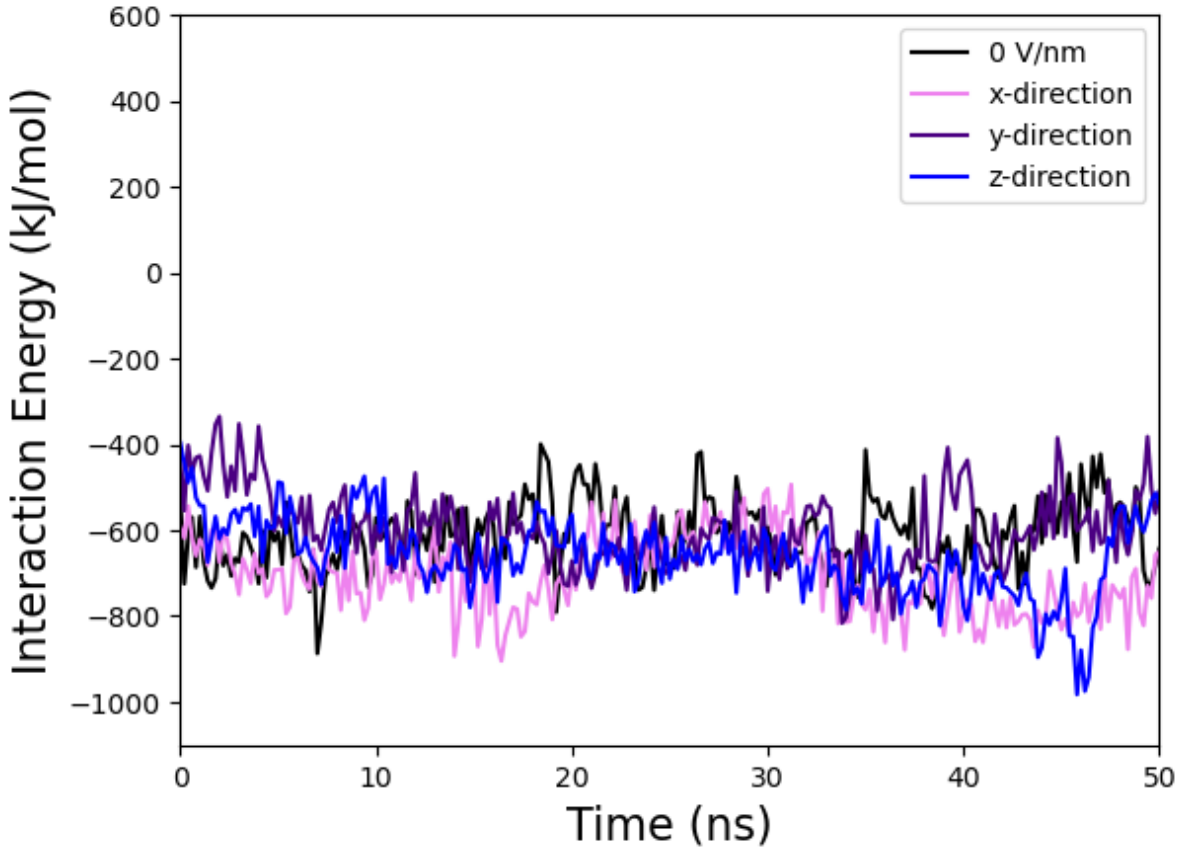

vii. Fig 4c: Interaction energy between the integrin and fibronectin when an electric field of 5 MV/m is applied from different directions.

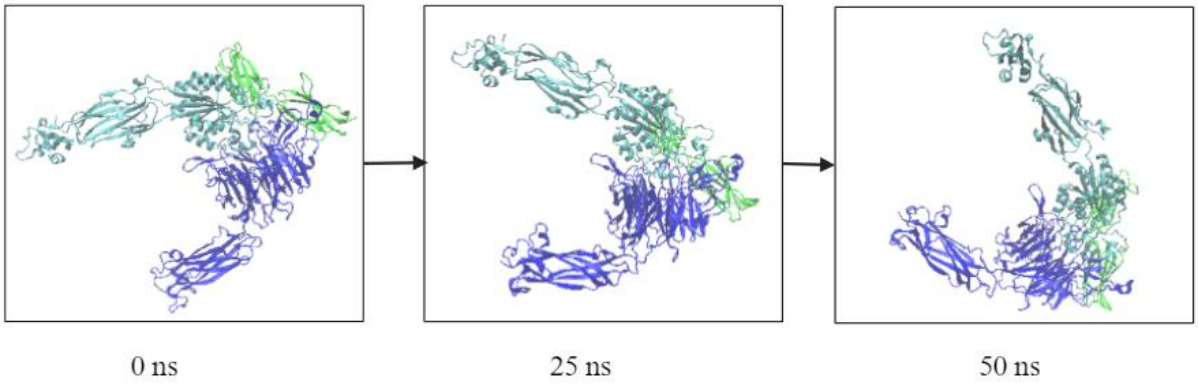

viii. Fig 5: Tumbling of the whole protein assembly observed when 5 MV/m electric field is applied in the x-direction. The fibronectin is depicted green, and the integrin subunits are blue and cyan. (Created in BioRender.com)

To further elaborate on this behaviour, the quantities were calculated at a slightly higher electric field strength of 10 MV/m. As seen in Fig 6, the RMSD values of both the integrin and fibronectin again did not vary much with direction and stayed consistently close to 0 nm over the course of the simulation. Here however, there

was a slightly higher RMSD observed in between the simulation from ~20 to ~45 ns when the electric field was applied in the y-direction. Again, there was a slightly higher variation in the interaction energies observed between the integrin and fibronectin. Observing the screenshots as seen in Fig 7, it can be seen that the same kind of tumbling can be observed for the whole protein when observing the run with an electric field in the y-direction.

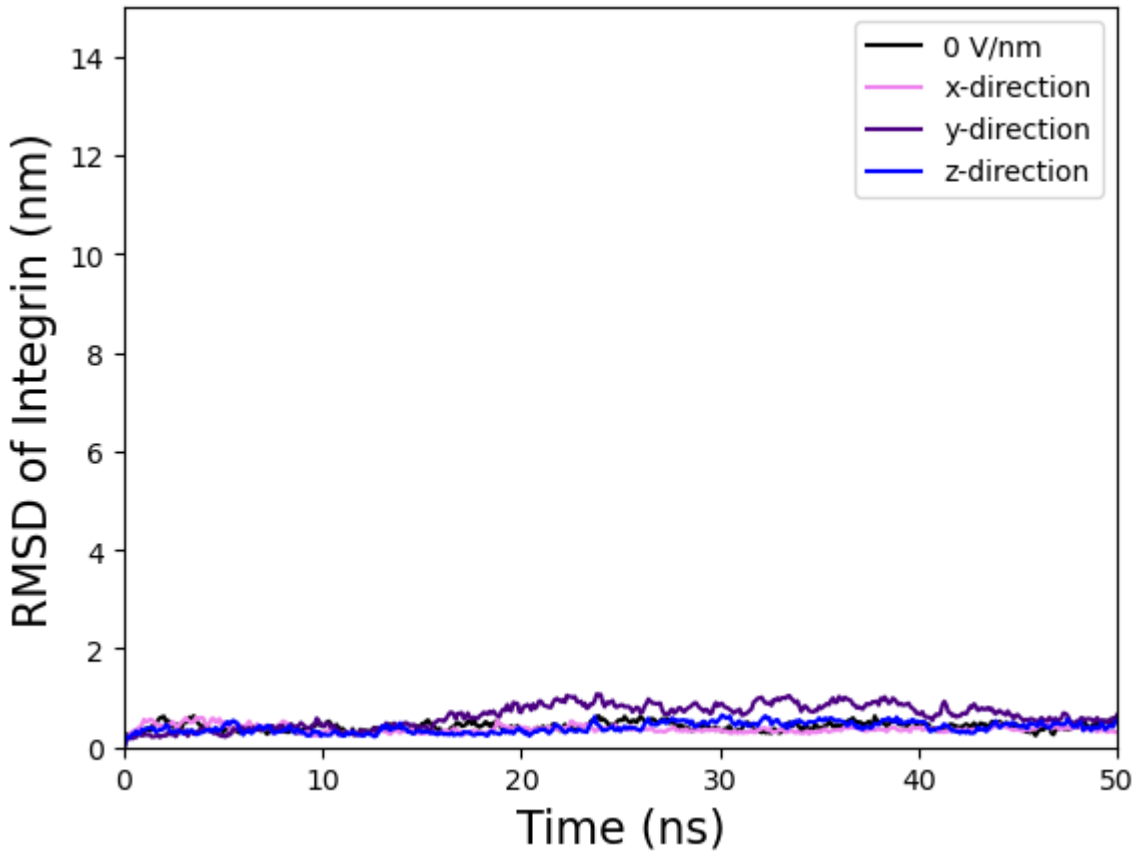

ix. Fig 6a: RMSD values of the integrin when an electric field of 10 MV/m is applied in three different directions.

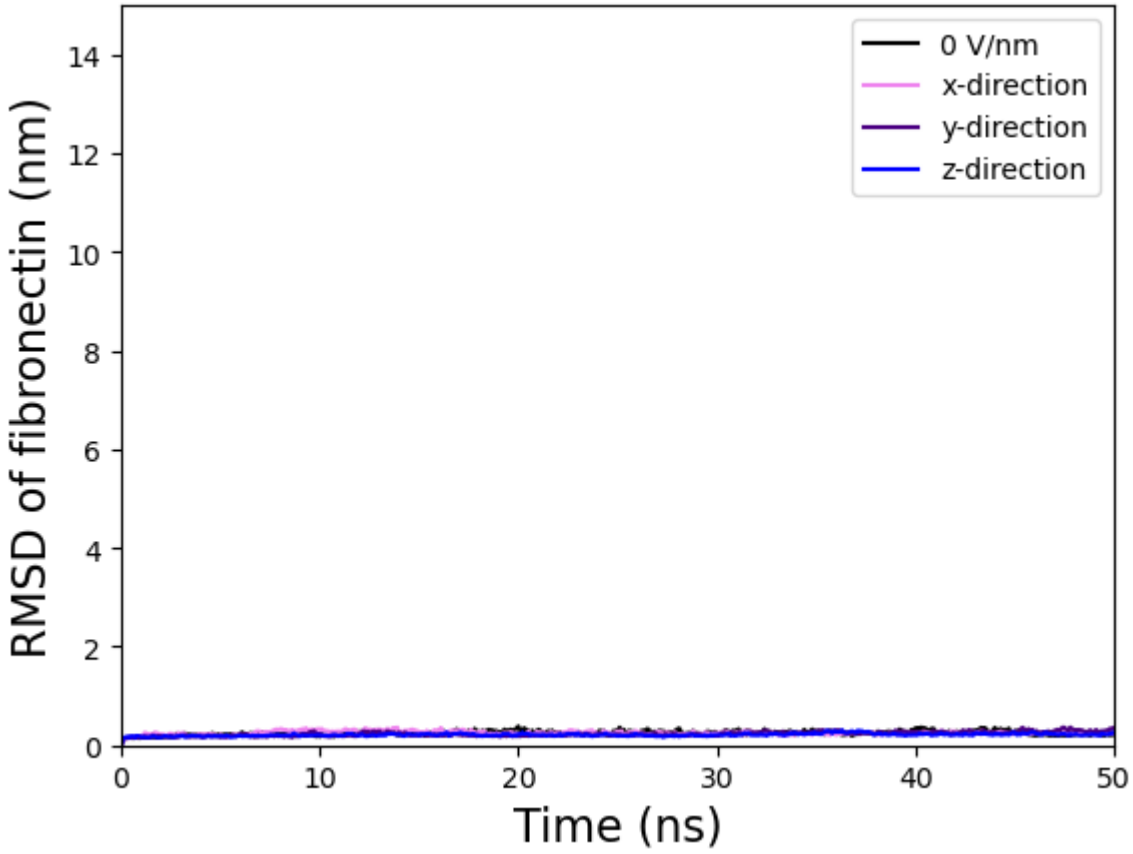

x. Fig 6b: RMSD values of fibronectin when an electric field of 10 MV/m is applied in three different directions.

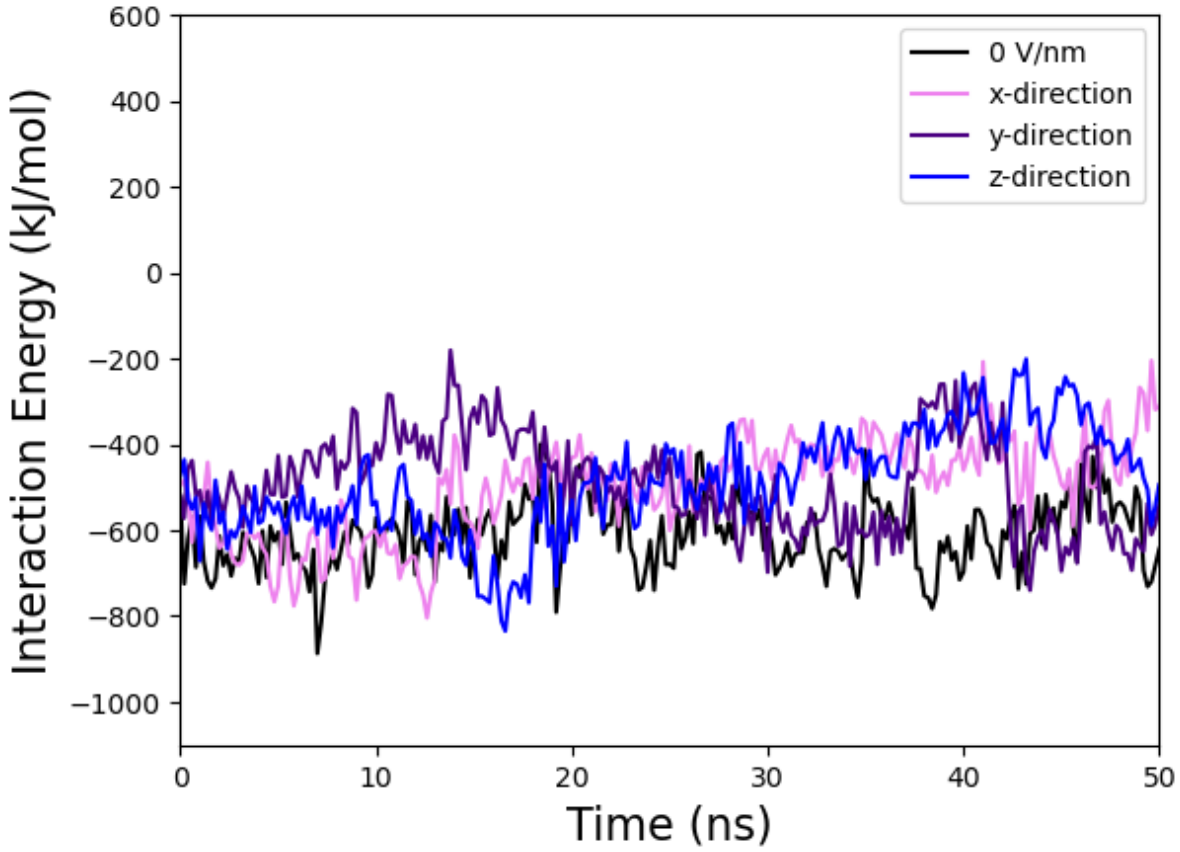

xi. Fig 6c: Interaction energy between the integrin and fibronectin when an electric field of 10 MV/m is applied from different directions.

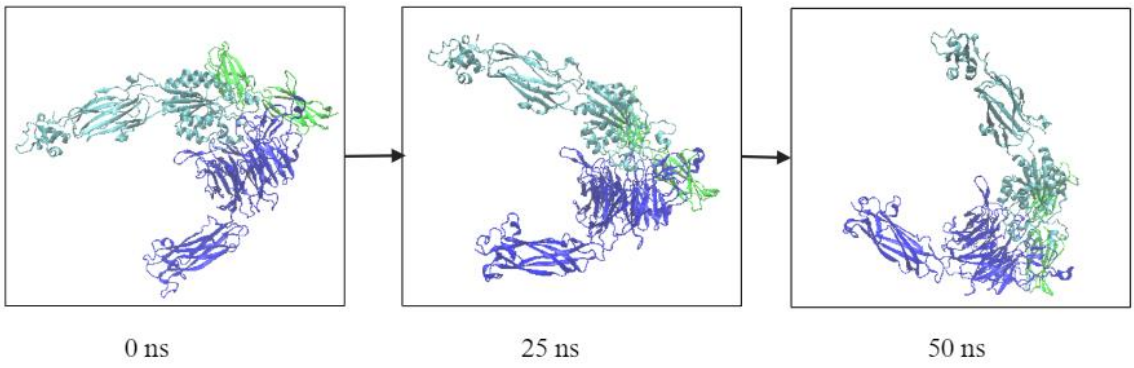

xii. Fig 7: Tumbling of the whole protein assembly observed when 10 MV/m electric field is applied in the y-direction. The fibronectin is depicted green, and the integrin subunits are blue and cyan. (Created in BioRender.com)

3.1.2 Variations with Electric Field Strength

In analysing the effects of an electric field with different field strengths, the Root Mean Square Deviations (RMSD) were calculated with respect to the initial structure separately for both the integrin and fibronectin From the RMSD of fibronectin it is clear that the protein denatures at electric fields of 500 and 1000 MV/m (Fig 8). The higher RMSD for 500 MV/m can be attributed to the stochasticity of such simulations, especially when the bonds present in the simulation are unstable. In the rest of the electric field strength values, the RMSD remains fairly low, indicating the stability of the fibronectin in the original cryo-EM structure, as seen in Fig 8, where the simulation with 0 electric field strength also showed similar stability. However, on the other hand, the RMSD of the integrin is also high for 500 and 1000 MV/m (Fig 8). But interestingly, for even lower electric field strengths from 50, 100 and 250 MV/m, the RMSD of integrin rises and falls back at some points (Fig 9). This can be attributed to the breakdown of the α_5 and β_1 subunits of the integrin as seen in the snapshots (Fig 9) For lower electric field strengths, the RMSD remains fairly low as expected (Fig 9).

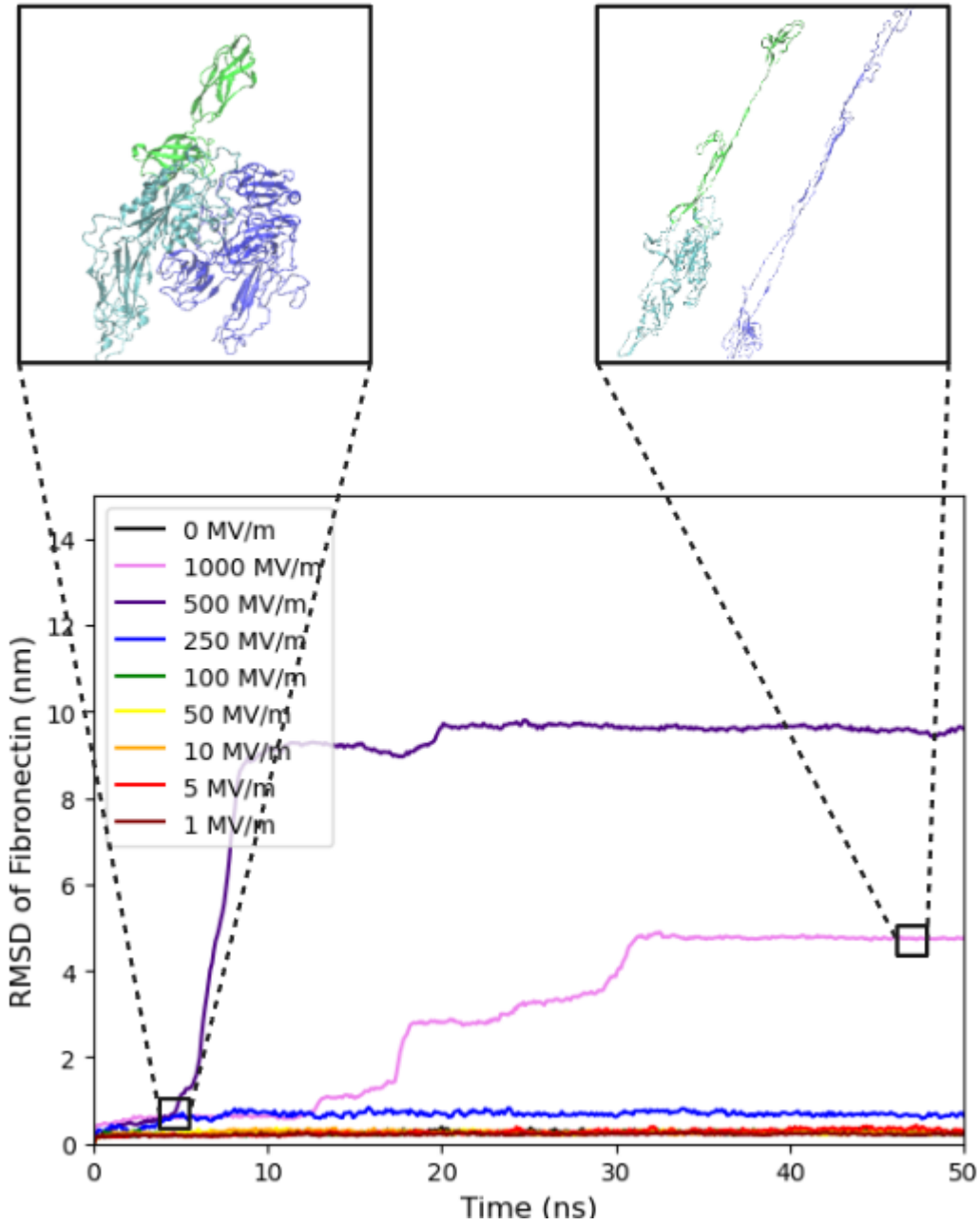

xiii. Fig 8: Variation of RMSD of Fibronectin with time, for different electric field strengths, with VMD snapshots for an electric field strength of 1000 MV/m (Created in BioRender.com)

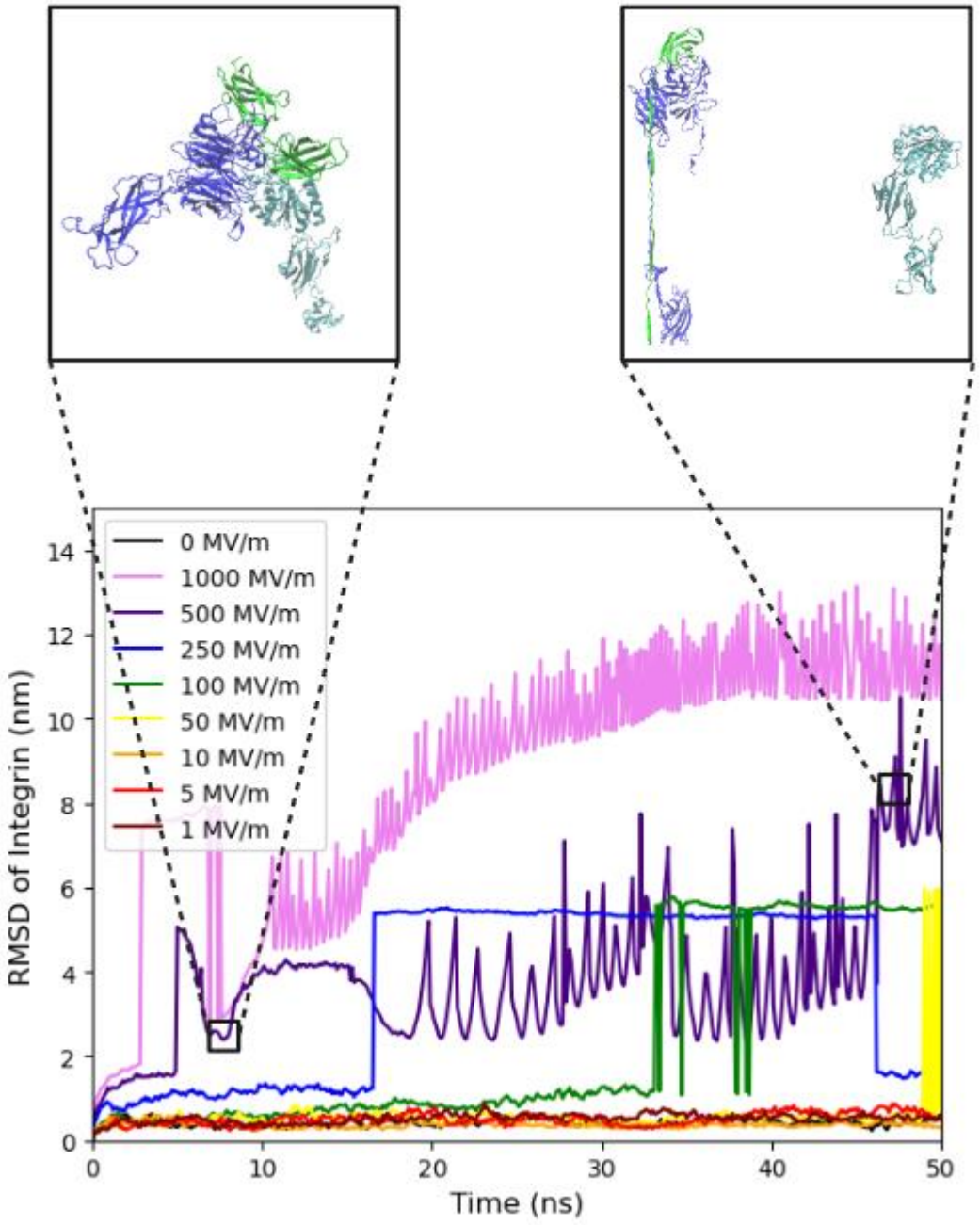

xiv. Fig 9: Variation of RMSD of Integrin with time, for different electric field strengths, with VMD snapshots for an electric field strength of 500 MV/m (Created in BioRender.com)

Moving on to the Integrin-Fibronectin Centre of Mass (COM) distance, we can again see the patterns of denaturation for higher electric fields of 500 – 1000 MV/m. Here, we can also see the electric field strengths at which the integrin and the fibronectin proteins dissociate, as can be seen by the higher COM distances between the integrin and fibronectin at some points of time (see Fig 10), for electric field strengths of 50 – 250 MV/m. We can also see that there is a difference between the levels of

dissociation at different electric fields, evident by the increased COM distance for higher electric fields in the range, as seen in Fig 11. Again, for lower electric field strengths, there is not much fluctuation in COM distance, indicating stability in binding and no dissociation as seen in Fig 7. To elaborate on the points of the above case, the COM distance between the α_5 and β_1 subunits of the integrin were also calculated. As expected, the higher electric fields of 500 and 1000 MV/m indicate high instability of the protein due to their highly oscillating COM distances. For lower electric field strengths and at 0 field strength, not much temporal variation in the COM distances were observed, indicating stability of the $\alpha_5\beta_1$ integrin complex, as shown in Fig 12.

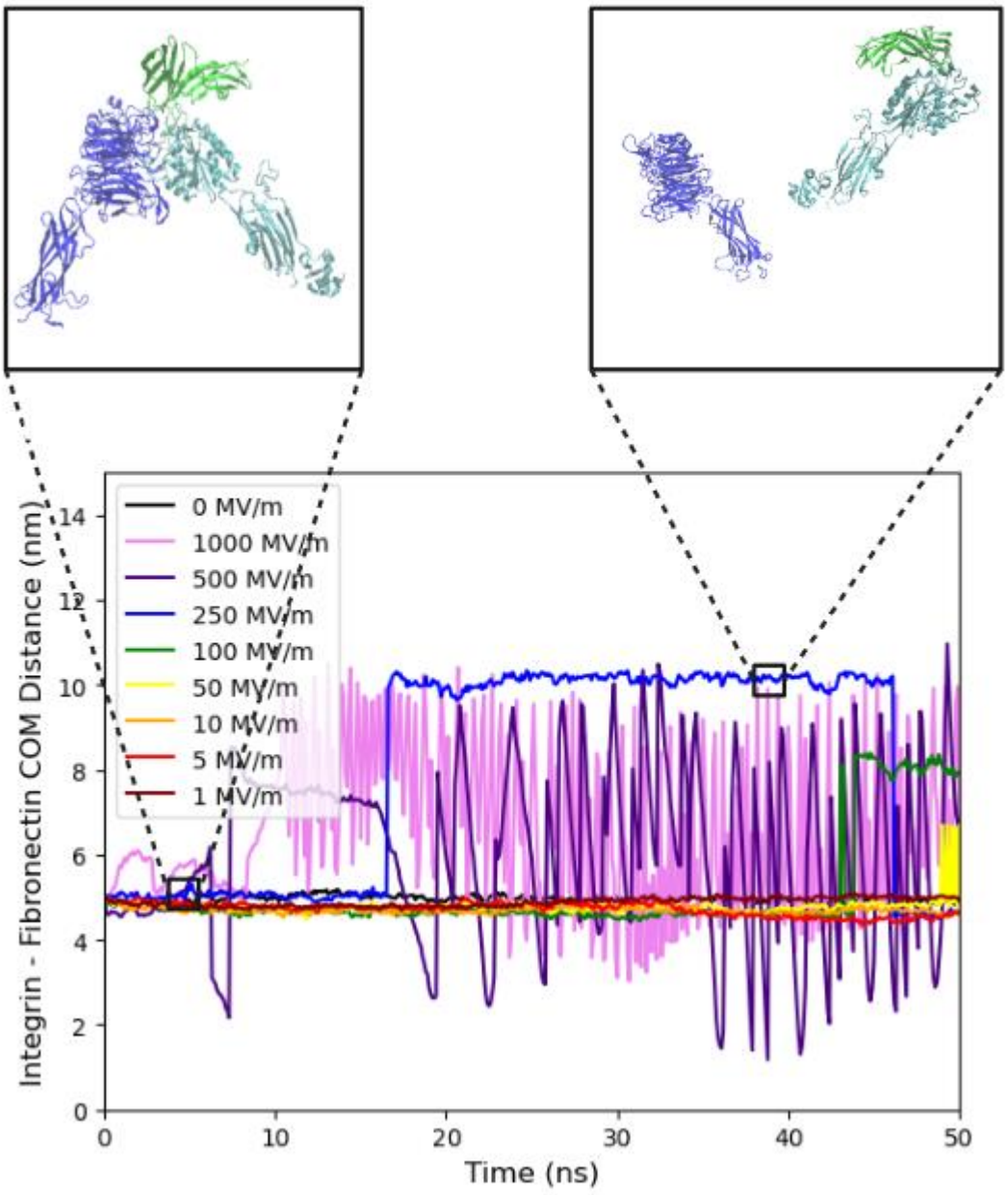

xv. Fig 10: Variation of Centre of Mass Distance between Fibronectin and the integrin with time, for different electric field strengths, with VMD snapshots for an electric field strength of 250 MV/m (Created in BioRender.com)

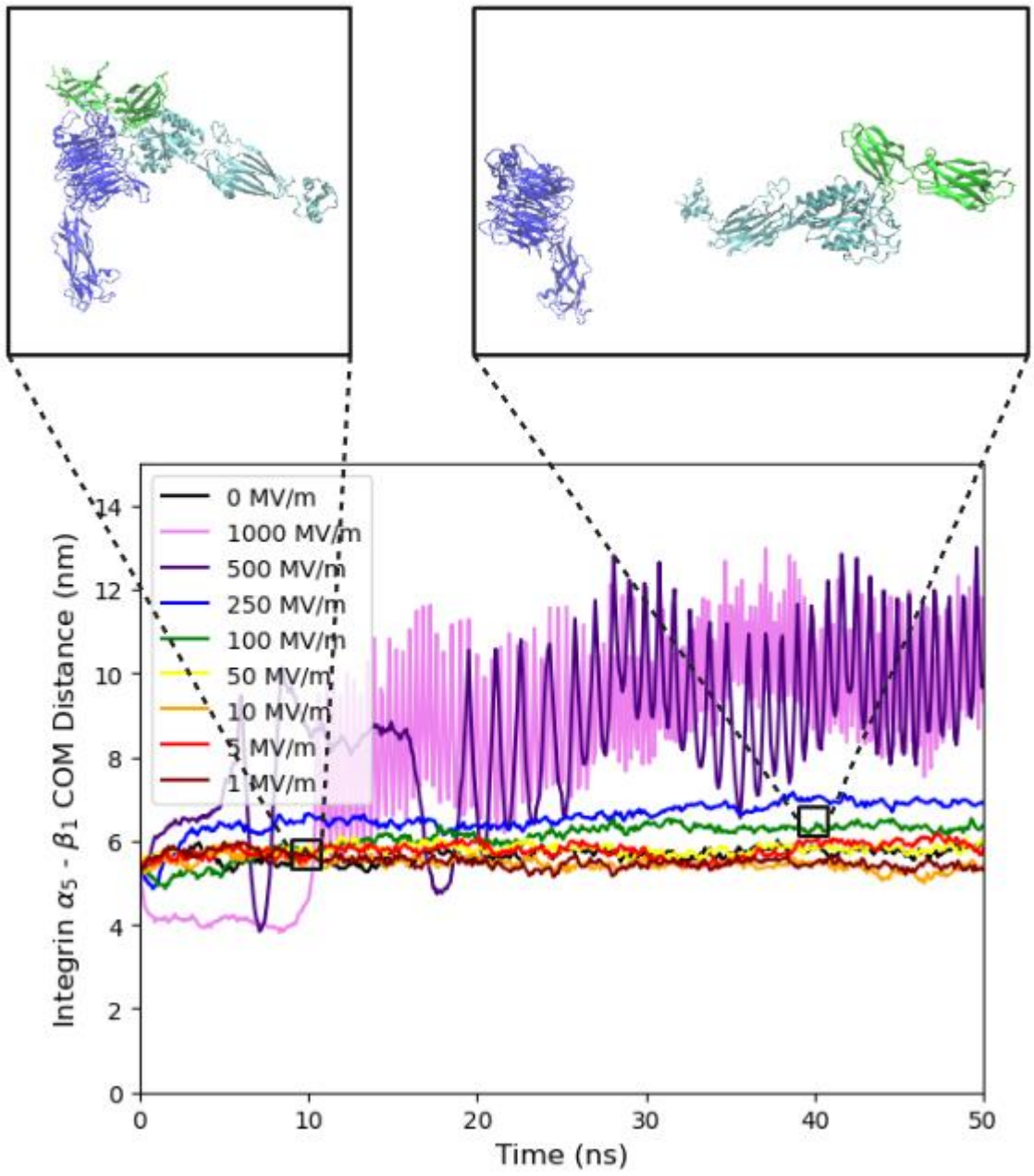

xvi. Fig 11: Variation of Centre of Mass distance between the α5 and β1 subunits with time, for different electric field strengths, with VMD snapshots for an electric field strength of 100 MV/m (Created in BioRender.com)

Finally, the interaction energy between the fibronectin and integrin was calculated. In harmony with the previous observations, temporal evolution of the interaction energies showed the instability in binding at high electric fields of 500 – 1000 MV/m due to denaturation. At lower electric fields, from 10 to 250 MV/m, there was much stable binding that was observed, since the values went 200 – 400 kJ/mol lower than that with 0 MV/m. However, at even lower electric field strengths of 1 – 5 MV/m, the interaction energy was as low as -1000 kJ/ mol, which is much lower than the

baseline interaction energy, in the absence of an electric field, where the total interaction energy only went as low as about -800 kJ/ mol, as seen in Fig 10.

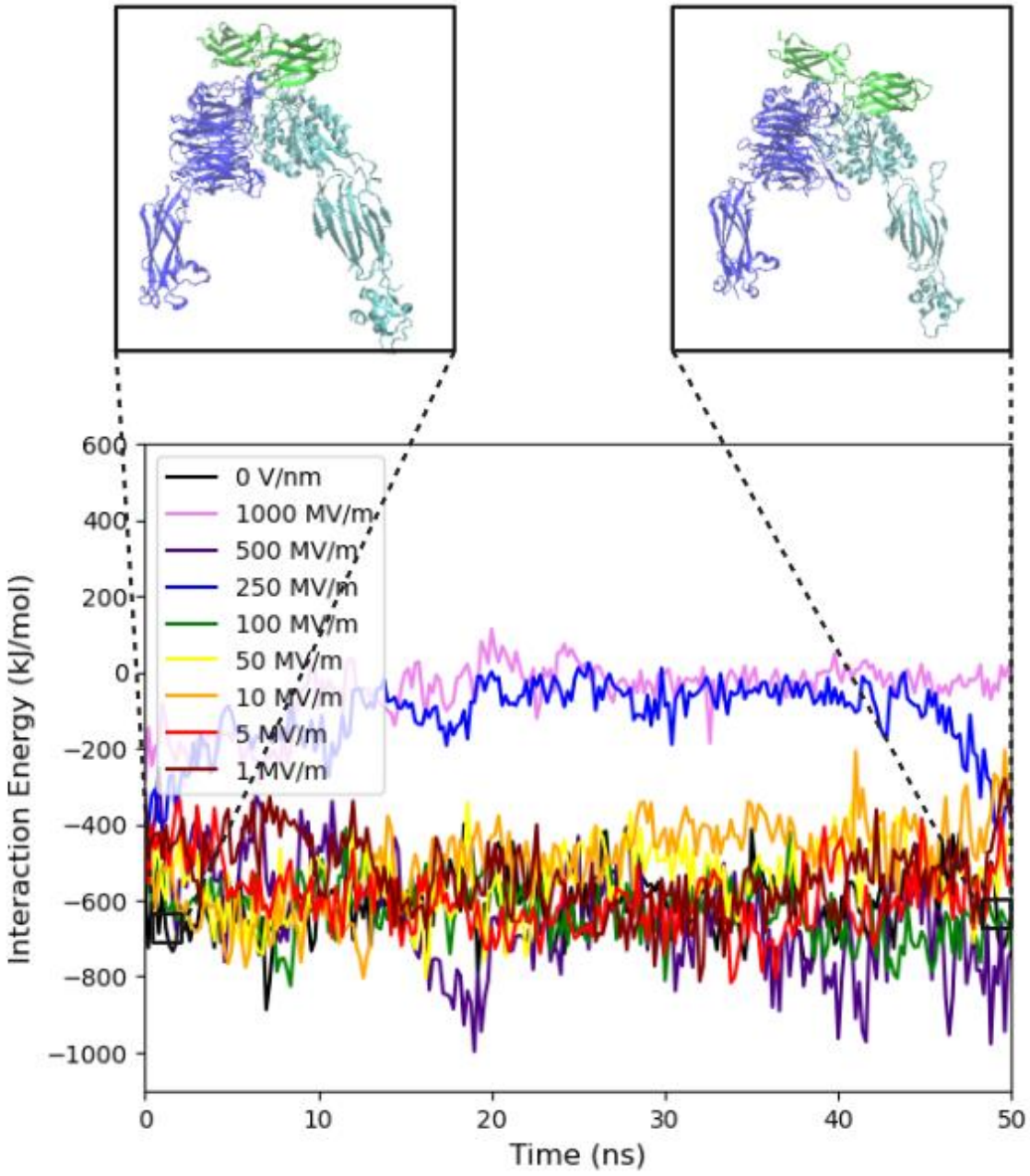

xvii. Fig 12: Variation of the interaction energy between the integrin and fibronectin, for different electric field strengths, with VMD snapshots for an electric field strength of 1 MV/m (Created in BioRender.com)

3.2 Focal Adhesion Complexes

For the kinetics simulation, major results such as the maturation factor and actin retrograde velocity were calculated with the optimal parameters following the work by Honasoge et al.[29] The simulation was conducted for a total timespan of 20 minutes, with the electric field being applied after the 10 min mark. Later, a local sensitivity analysis was also performed to determine the sensitivity of the results with respect to the estimated, non-experimental parameters that were taken into account. This was done to establish the validity of the obtained results through a variety of values of such parameters, and also to establish the robustness of the model predictions.

For the maturation factor, it was observed that the total maturation factor, which describes the total number of NAs maturing into FAs did not vary with a change in electric field. This was expected, because the original governing equations had a mass conservation term included in them, which kept the total number of available vinculins for focal adhesions constant. However, among the FAs, it was observed that the mid order FAs, containing two vinculins were more favoured with a higher electric field strength. The higher order FAs were more favourable under lower and even in absence of electric field strength, as seen in Fig 13. In terms of the time evolution of FA formation, NAs form quickly with a peak at around 50s. But then, they all mature to FAs soon. By 10 mins, the maturation reaches a saturated state, and the electric field is then applied. This almost instantly changes the concentrations of Mid order and High order clutches, which again lets the total concentrations remain constant after the initial peak, as seen in Fig 13.

In terms of the total force experienced by the individual clutches, we can observe that the total variation in the forces experienced by the clutches was much higher when a much higher electric field was applied. This is also expected, since a higher addition to the initial force, due to the myosin motors, is also higher with a higher electric field.

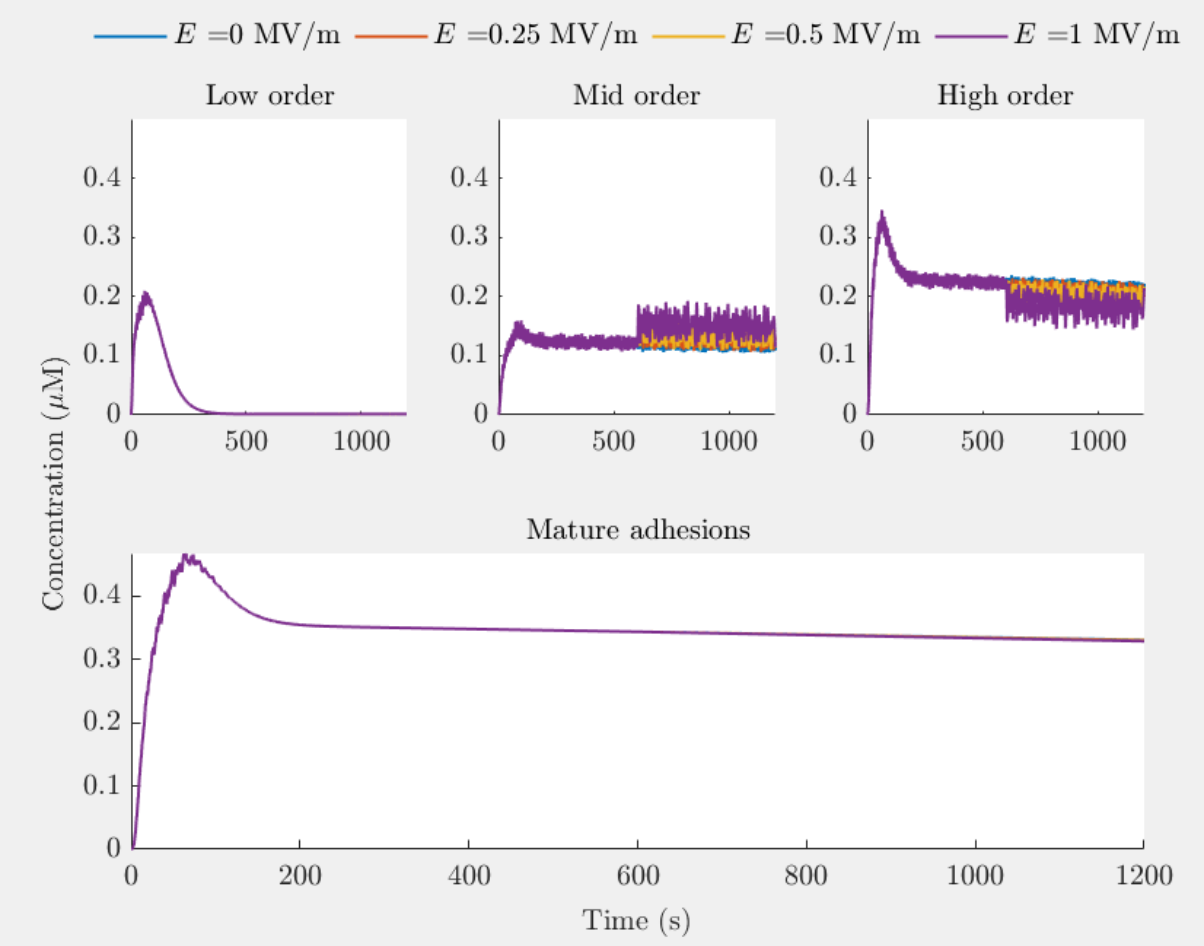

xviii. Fig 13: Variation of maturation of FAs with time ,for different electric field strengths.

In terms of the actin retrograde velocity, we can observe that there is a steady increase in the values when increasing electric field strength from 88 nm/s at 0 MV/m to about 94 nm/s at 1 MV/m. As mentioned earlier, this indicates a higher traction force with a higher electric field intensity will be experienced by the cell, as seen in Fig 14.

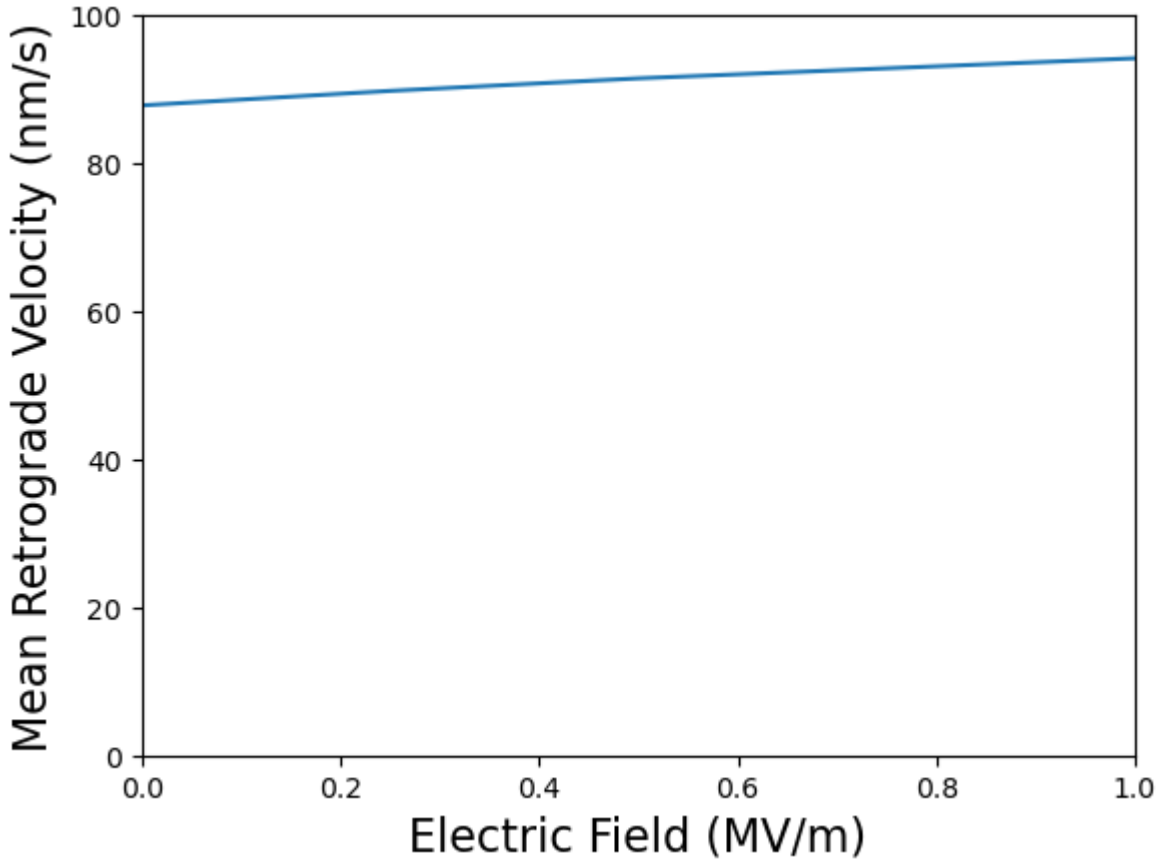

xix. Fig 14: Variation of the mean actin retrograde velocity with increasing electric field strength

3.2.1 Sensitivity Analysis

For the sensitivity analysis, various parameters were considered. Table 2 contains all the initial values of the parameters analysed for the sensitivity analysis.

Parameter	Definition	Initial Value
v_u	Initial actin retrograde velocity	10 nm/s
k_{tal}	Stiffness of talin	0.25 pN/nm
$Initial_{vinc}$	Initial concentration of vinculin	1 μM
$Initial_{int}$	Initial concentration of integrins	1 μM
k_{sens}	Time dependency factor	0.05
k_{act}	Baseline actin binding rate	1.5 s^{-1}
tal_{rf}	Talin refolding rate	1 s^{-1}
$tal_{rf\ factor}$	Initial talin refolding rate modifying factor	0.5

Table 2: Initial baseline parameters and their values considered for the sensitivity analysis

These parameters were varied in percentages from +20% to -20%. As seen in Fig 15, the actin loading rate and the initial vinculin concentration are the major contributors to the sensitivity of the system.

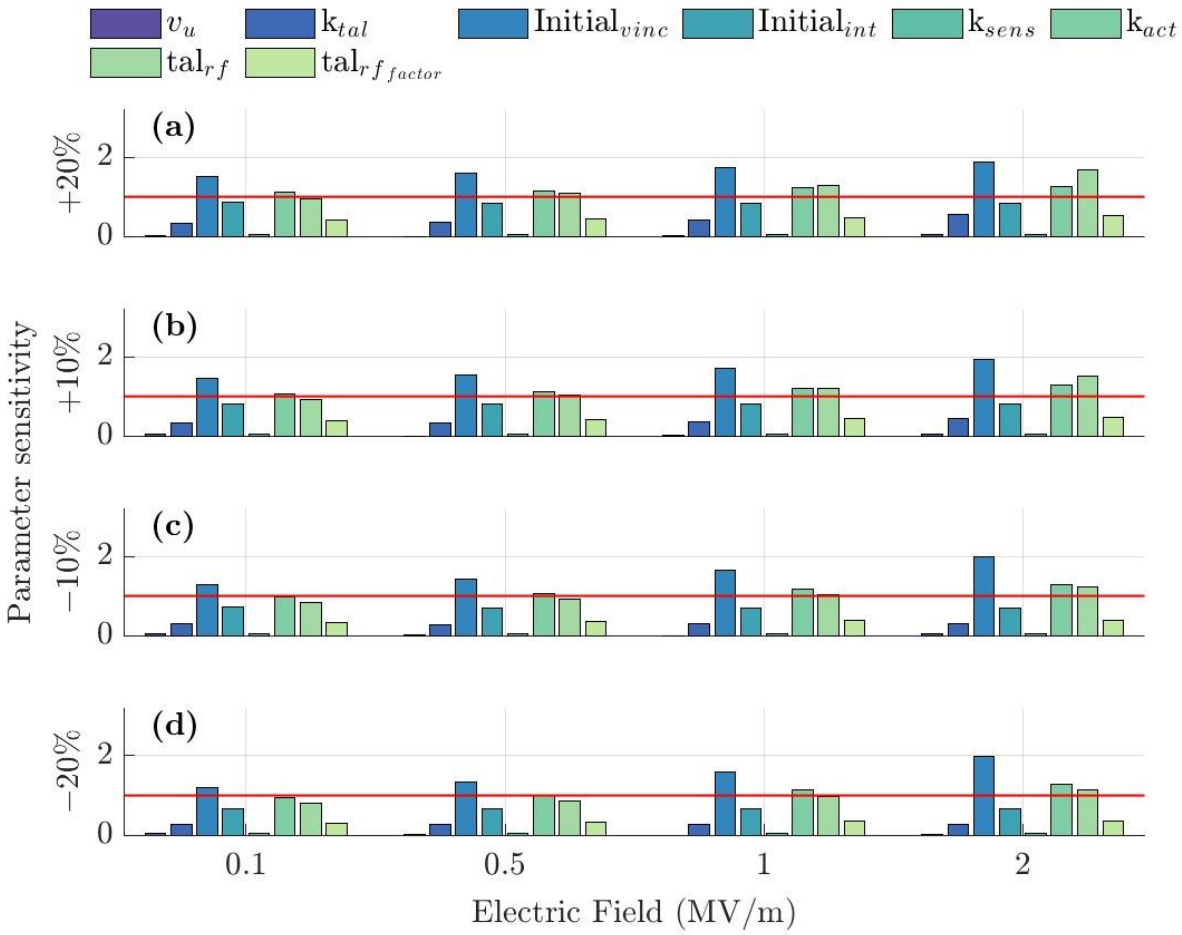

xx. Fig 15: Sensitivity analysis of various parameters in the model and their effect over different electric field strengths

In analysing the effects of these parameters on the final actin retrograde velocity, the initial estimated actin retrograde velocity played a major role in the sensitivity of the model towards the final retrograde velocity, regardless of the electric field value, as expected. For a -20% value, the retrograde velocity peaked around 80 nm/s while for a higher initial value of +20%, the actin retrograde velocity peaked around 120 nm/s. However, all the other parameters converged 2 MV/m, showing the robustness of the model towards various parameters as seen in Fig 16. The variation of the velocity with k_{tal} varied from 80 nm/s with -20% to close to 100 nm/s for a +20% variation at 0 MV/m but again converged at 2 MV/m. $Initial_{vinc}$ and k_{act} had similar effects on the retrograde velocity. With a -20% variation, the retrograde velocity was close to 80 nm/s close and a +20% variation resulted in a retrograde velocity of about 95 nm/s at 0 MV/m. At high electric field strengths of 2 MV/m, they converged to about 105 MV/m. $Initial_{int}$ and tal_{rf} however, had a lesser effect on the same quantities with the range from 85 – 95 nm/s at 0 MV/m and a better convergence at 2 MV/m to 105

nm/s. The variations in the remaining parameters k_{sens} and $tal_{rf\ factor}$ had almost no impact on the actin retrograde velocity and was very similar to the baseline values as seen in Fig 16.

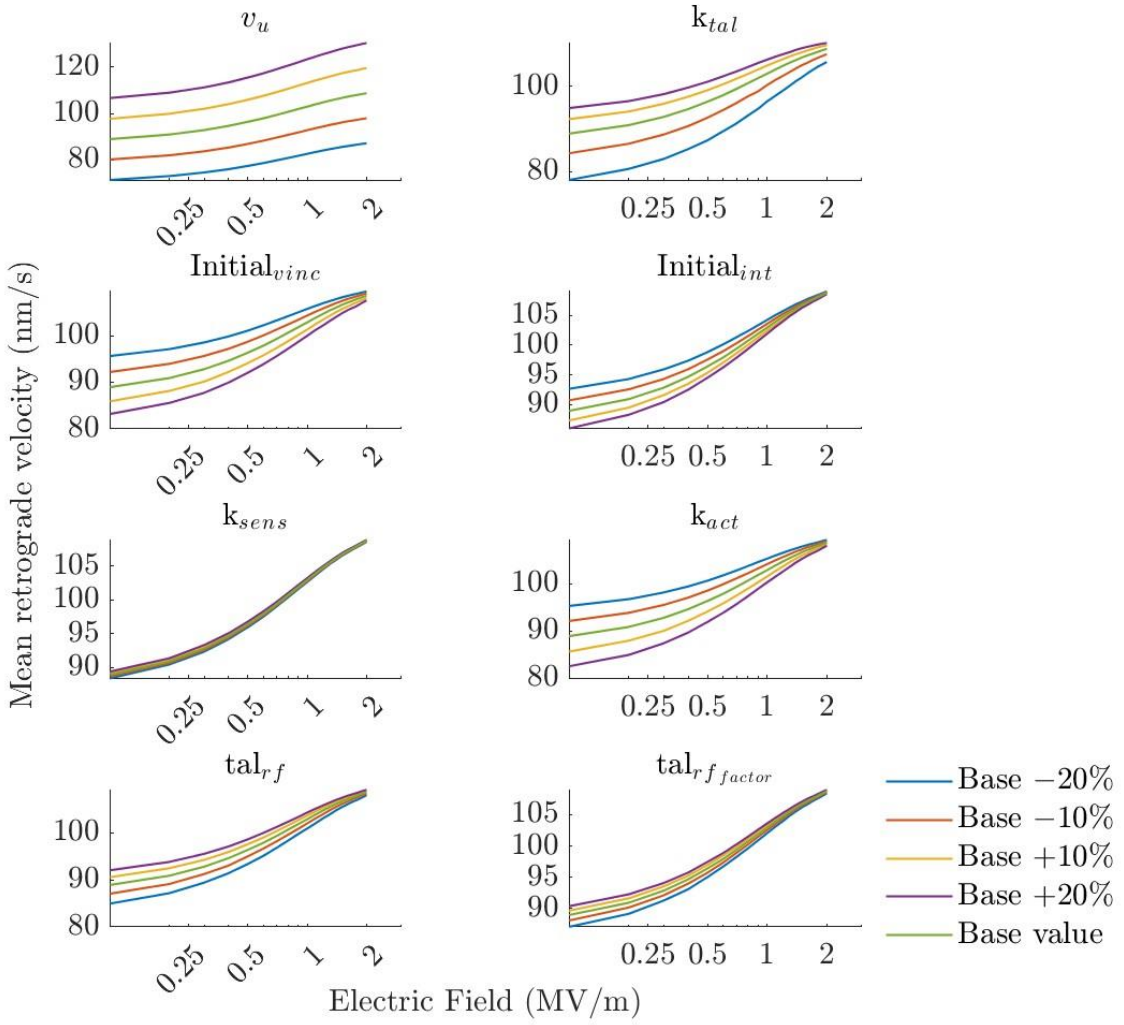

xxi. Fig 16: Variation of the mean actin retrograde velocity, while varying the sensitivity of different parameters in the sensitivity analysis of the original model.

Chapter 4 Discussion

The discussion in this section will centre around uncovering the role of electric field on fibronectin – integrin interactions at a small timescale (< 50 ns) as well as intracellular biophysical interactions among the key proteins in relation to the cytoskeletal reorganization. The computational simulation work, presented in the preceding section can be better rationalized against earlier studies from our own group. Experimentally, we demonstrated the phenotypical changes of stem cells with cytoskeletal reorganization and gene regulatory protein regulation, confirming osteogenesis, neurogenesis or cardiomyogenesis under electric field stimulation[5, 6]. In some cases, we also reported the cell migration enhancement, as confirmed using the scratch array, under electric field stimulation.

In analysing the MD simulation results, we note that the interactions between the integrin and fibronectin proteins is extremely stable at lower electric field strength. In fact, at E<10 MV/m, the interaction energy between the two proteins was lower than that in the absence of an electric field by about 200 kJ/mol. In the presence of moderately higher electric field strengths up to 250 MV/m, was some separation between the integrin and the fibronectin was recorded, as visualised using both the VMD simulations and RMSD diagrams. In the presence of much higher electric fields (500 – 1000 MV/m), both the proteins denature at such high electric fields. While it is possible that denaturation happens at lower external electric fields as well, the observations made are valid to the small timescale of 50 ns. In fact, the whole protein tumbled and rotated to align with the lowest possible energy direction, when the field was applied in different directions. These observations indicate a strong electrostatic attractive force between the integrin and the fibronectin, which requires a very high electric field strength to break. Our results also indicate that the binding of the two proteins can be stabilized more under an appropriate electric field strength. This is possible due to the high electrostatic affinity of the RGD loop to the metal-ion sites, as has been observed experimentally in previous studies as well.

Earlier works were done in the lab by Basu, S et al[13]. which investigated the effects of an external electric field on fibronectin – biomaterial (hydroxyapatite) interactions. They mostly observed interactions at a higher range of electric fields from 100 – 1000 MV/m. However, in the current work, at such similar electric fields, it was

observed that the whole protein either denatured, or the binding was not stable. Since the system sizes in both studies were vastly different, it is hard to compare them quantitatively in terms of quantities like interacting energy. But in terms of qualitative results, we can say that both these studies help to qualitatively establish the dynamics of the overall process of electric field stimulation on a cell-material interface, such as the importance of the RGD loop in binding.

Actin retrograde velocity increased with increase in electric field. One possible explanation for this is that the electric field increased the traction force on the cell, thus resulting in better motility of the focal adhesions. On the other hand, it was also seen that the higher order vinculins were more favoured with a lower electric field strength. This might be another mechanism through which an external electric field reduces the stability of focal adhesions, thus helping in cell motility.

Overall, the work improved on our understanding of the process of electric field stimulation of cells on a biomaterial surface. While at very high electric field strengths, the cell motility is improved at the expense of protein denaturation. Hence, even though high electric field strengths are good in terms of actin retrograde velocity, which can influence many downstream processes, care must be taken so that the stability of these adhesions are not compromised.

References

[1] Hynes, R. O. (1987). Integrins: a family of cell surface receptors. *cell*, *48*(4), 549-554.

[2] Kumar, C. C. (1998). Signaling by integrin receptors. Oncogene, 17(11), 1365-1373.

[3]Ahmad Khalili, A., & Ahmad, M. R. (2015). A review of cell adhesion studies for biomedical and biological applications. International journal of molecular sciences, 16(8), 18149-18184.

[4] Ravikumar K., B. Sunilkumar and Bikramjit Basu; Synergy of substrate conductivity and intermittent electrical stimulation towards osteogenic differentiation of human mesenchymal stem cells, Bioelectrochemistry 116 (2017) 52–64.

[5] Greeshma Thrivikraman, P. Lee, R. Hess, V. Haenchen; Bikramjit Basu; D. Scharnweber. Interplay of substrate conductivity, cellular microenvironment and pulsatile electrical stimulation towards osteogenesis of human mesenchymal stem cells *in vitro*; ACS Applied Materials & Interfaces 7[41] (2015) 23015–23028.

[6] A. K. Dubey and B. Basu; Pulsed electrical stimulation and surface charge induced cell growth on multistage spark plasma sintered hydroxyapatite-barium titanate piezobiocomposite; J. Am. Cer. Soc. 97[2] (2014) 481-489.

[7] Ashutosh Dubey, Shouriya Dutta Gupta and Bikramjit Basu; Optimization of electrical stimulation conditions for enhanced fibroblast cell proliferation on biomaterial surfaces; Journal of Biomedical Materials Research: Part B - Applied Biomaterials 98 B[1] (2011) 18–29.

[8] Nitu Bhaskar, Midhun C Kachapilly, Bhushan V, Hardik J. Pandya, Bikramjit Basu, Electrical field stimulated modulation of cell fate of pre-osteoblasts on PVDF/BT/MWCNT based electroactive biomaterials, Journal of Biomedical Materials Research A 111 [3] (2022) 340-353.

[9] Asish Kumar Panda, V. S. N. Sitaramgupta, H. J. Pandya, B Basu, Electrical stimulation waveform-dependent osteogenesis on PVDF/$BaTiO_3$ composite using a customized and programmable cell stimulator, Biotechnology and Bioengineering 119 [6] (2022)1578-1597.

[10] Greeshma Thrivikraman, Giridhar Madras, Bikramjit Basu, Electrically driven intracellular and extracellular nanomanipulators evoke neurogenic/cardiomyogenic differentiation in human mesenchymal stem cells. Biomaterials 77 (2016) 26-43.

[11] Greeshma Thrivikraman, Giridhar Madras and Bikramjit Basu; Intermittent electrical stimuli for guidance of human mesenchymal stem cell lineage commitment towards neural-like cells on electroconductive substrates; Biomaterials 35 (2014) 6219–6235.

[12] Ravikumar, K., Kumaran, V., & Basu, B. (2019). Biophysical implications of Maxwell stress in electric field stimulated cellular microenvironment on biomaterial substrates. Biomaterials, 209, 54-66.

[13] Basu, S., Basu, B., & Maiti, P. K. (2022). A computational study on strontium ion modified hydroxyapatite–fibronectin interactions. *Physical Chemistry Chemical Physics*, *24*(45), 27989-28002.

[14] Basu, B., Aditya, D., Kumaran, V., & Ravikumar, K. (2025). Biophysical insights into the impact of lateral electric field stimulation to cellular microenvironment: Implications for Bioelectronic medicine applications. *Biomaterials*, 123132.

[15] Abasi, S., Jain, A., Cooke, J. P., & Guiseppi-Elie, A. (2023). Electrically stimulated gene expression under exogenously applied electric fields. *Frontiers in Molecular Biosciences*, *10*, 1161191.

[16] Naskar, S., Kumaran, V., Markandeya, Y. S., Mehta, B., & Basu, B. (2020). Neurogenesis-on-Chip: Electric field modulated transdifferentiation of human mesenchymal stem cell and mouse muscle precursor cell coculture. *Biomaterials*, *226*, 119522.

[17] Cheng, Bo, Min Lin, Guoyou Huang, Yuhui Li, Baohua Ji, Guy M. Genin, Vikram S. Deshpande, Tian Jian Lu, and Feng Xu. "Cellular mechanosensing of the biophysical microenvironment: a review of mathematical models of biophysical regulation of cell responses." *Physics of life reviews* 22 (2017),88-119.

[18] Cheng, B., Li, M., Wan, W., Guo, H., Genin, G. M., Lin, M., & Xu, F. (2023). Predicting YAP/TAZ nuclear translocation in response to ECM mechanosensing. *Biophysical journal*, *122*(1), 43-53.

[19] Schumacher, S., Dedden, D., Nunez, R. V., Matoba, K., Takagi, J., Biertümpfel, C., & Mizuno, N. (2021). Structural insights into integrin α5β1 opening by fibronectin ligand. *Science Advances*, *7*(19), eabe9716.

[20] Kapp, T. G., Rechenmacher, F., Neubauer, S., Maltsev, O. V., Cavalcanti-Adam, E. A., Zarka, R., ... & Kessler, H. (2017). A comprehensive evaluation of the activity and selectivity profile of ligands for RGD-binding integrins. *Scientific reports*, *7*(1), 1-13.

[21] Jo, S., Kim, T., Iyer, V. G., & Im, W. (2008). CHARMM-GUI: a web-based graphical user interface for CHARMM. *Journal of computational chemistry*, *29*(11), 1859-1865.

[22] Brooks, B. R., Brooks III, C. L., Mackerell Jr, A. D., Nilsson, L., Petrella, R. J., Roux, B., ... & Karplus, M. (2009). CHARMM: the biomolecular simulation program. *Journal of computational chemistry*, *30*(10), 1545-1614.

[23] H. Bekker, H.J.C. Berendsen, E.J. Dijkstra, S. Achterop, R. van Drunen, D. van der Spoel, A. Sijbers, and H. Keegstra et al., “Gromacs: A parallel computer for molecular dynamics simulations”; pp. 252–256 in Physics computing 92. Edited by R.A. de Groot and J. Nadrchal. World Scientific, Singapore, 1993.

[24] Bussi, G., Donadio, D., & Parrinello, M. (2007). Canonical sampling through velocity rescaling. *The Journal of chemical physics*, *126*(1).

[25] Bernetti, M., & Bussi, G. (2020). Pressure control using stochastic cell rescaling. *The Journal of Chemical Physics*, *153*(11).

[26] Hess, B., Bekker, H., Berendsen, H. J., & Fraaije, J. G. (1997). LINCS: A linear constraint solver for molecular simulations. *Journal of computational chemistry*, *18*(12), 1463-1472.

[27] Hopkins, C. W., Le Grand, S., Walker, R. C., & Roitberg, A. E. (2015). Long-time-step molecular dynamics through hydrogen mass repartitioning. *Journal of chemical theory and computation*, *11*(4), 1864-1874.

[28] Wang, J., Wolf, R. M., Caldwell, J. W., Kollman, P. A., & Case, D. A. (2004). Development and testing of a general amber force field. *Journal of computational chemistry*, *25*(9), 1157-1174.

[29] Humphrey, W., Dalke, A., & Schulten, K. (1996). VMD: visual molecular dynamics. *Journal of molecular graphics*, *14*(1), 33-38.

[30] Honasoge, K. S., Karagöz, Z., Goult, B. T., Wolfenson, H., LaPointe, V. L., & Carlier, A. (2023). Force-dependent focal adhesion assembly and disassembly: A computational study. *PLoS Computational Biology*, *19*(10), e1011500.

[31] Swaminathan, V., & Waterman, C. M. (2016). The molecular clutch model for mechanotransduction evolves. *Nature cell biology*, *18*(5), 459-461.